

RESEARCH

Open Access



# Computational investigation, virtual docking simulation of 1, 2, 4-Triazole analogues and insillico design of new proposed agents against protein target (3IFZ) binding domain

Shola Elijah Adeniji<sup>1\*</sup> , David Ebuka Arthur<sup>2</sup>, Mustapha Abdullahi<sup>1</sup> and Olajumoke Bosede Adalumo<sup>3</sup>

## Abstract

**Background:** The reoccurrence of the resistant strains of *Mycobacterium tuberculosis* to available drugs/medications has mandated for the development of more effective anti-tubercular agents with efficient activities. Therefore, this work utilized the application of modeling technique to predict the inhibition activities of some prominent compounds which been reported to be efficient against *M. tuberculosis*. To accomplish the purpose of this work, multiple regression and genetic function approximation were adopted to create the model.

**Results:** The established model was swayed with topological descriptors: MATS7s, SM1\_DzZ, TDB3v, and RDF70v. More also, interactions between the compounds and the target "DNA gyrase" were evaluated via docking approach utilizing the PyRx and Discovery Studio simulated software. Meanwhile, compound 19 has the most perceptible binding affinity of  $-16.5$  kcal/mol. Consequently, compound 19 served as a reference structural template and insight to design twelve novel hypothetical agents with more competent activities. Meanwhile, compound 19h was observed with high activity among the designed compounds with more prominent binding affinities of  $-21.6$  kcal/mol.

**Conclusion:** Therefore, this research recommends in vivo, in vitro screening and pharmacokinetic properties to be carried out in order to determine the toxicity of the designed compounds.

**Keywords:** Model, Triazole QSAR, Tuberculosis

## Background

The World Health Organization (WHO) has declared tuberculosis as a major health issue to date. Despite its descending trend in prevalence and occurrence, new cases were still reported by every continent particularly in Southeast Asia and Africa. The WHO, in 2017, reported 9 million of who get infected and mortality rate of 1.6 million people globally (W.H.O 2018).

Anti-tubercular drugs recommended for treating tuberculosis include the following: rifampicin, pyrazinamide, para-aminosalicylic acid, and isoniazide (Adeniji et al. 2020a). However, reports have shown that patients do not respond positively to the administered drugs due to the resistance strain of *Mycobacterium tuberculosis* toward the current drugs. More also, most of these drugs have been reported with adverse side effect (Adeniji et al. 2020a). Therefore, the pursuit of novel anti-tubercular agents with enhanced and efficient properties/activities with minimum side effects against

\* Correspondence: [shola4343@gmail.com](mailto:shola4343@gmail.com)

<sup>1</sup>Chemistry Department, Ahmadu Bello University, Zaria, Kaduna State 810107, Nigeria

Full list of author information is available at the end of the article

*M. tuberculosis* still remains a challenge to pharmacist and chemists (Adeniji et al. 2020b).

A type II topoisomerase target “DNA gyrase (3IFZ)” is present in all bacteria. It produces negative supercoils for the whole bacterial chromosome which relaxes the supercoils that generate the translocating RNA polymerase which shortened the chromosome for appropriate segregation during cell division (James 2009; Huang et al. 2006). This enzyme is a tetramer that is made up of “two subunits A” which comprises the DNA binding domain and “two subunits B” which catalyzes the reaction that quickly cleaves two DNA strands which depend on ATP hydrolysis. The two subunits A and B, i.e., GyrA and GyrB, aid the DNA replication by breaking and reuniting the DNA strand. Based on the function stated, the termination of the DNA replication can be blocked by prominent inhibitors targeting either the GyrA (DNA domain) or the GyrB (ATP binding cavities).

Heterocyclic molecules have been conventionally developed and established to play vital roles in medicinal applications due to their structural entities (Zhang et al. 2006). Triazole and its analogue among all other heterocyclic compounds are being considered in pharmacological fields due to its unique structure and properties (Adeniji et al. 2020b; Zhang et al. 2006). Triazole is a five-membered ring heterocyclic diunsaturated compound composed of two carbon atoms at and three nitrogen atoms at non-adjacent positions, respectively. Recent researches have shown that triazole nucleus has gained huge attention among pharmacist, biochemist, biologist, and chemists as it is one of the major bioactive molecules in pharmaceuticals particularly in drug design and chemotherapeutic (Holla et al. 2005). Triazole has been reported to show substantial and extensive kind of pharmacological activities such as analgesic and anti-tubercular (<https://patents.justia.com/patent/8865910>, (Hafez et al. 2008)), anti-neoplastic (Guan et al. 2007), and anti-malarial (Gujjar et al. 2009). It is also reported as the most efficient molecules toward anti-TB activity (Patel et al. 2010).

For the time being, advancement of computational chemistry led to new challenges of drug discovery. Computational chemistry has made in silico methods to become widely used in the field of structure-based drug design which reduces the cost for effective evaluation of large virtual database of chemical compounds. Such computational method includes quantitative structure-activity relationships (QSARs) and molecular docking (Adeniji et al. 2020a).

The first stage is to design and synthesis novel hypothetical compounds with enhanced anti-tubercular activity and less toxicity/side effect with the approaches and methods that will consider the rate of experimental runs and time factor. Reference to the design of novel drug

candidate, computer-aided drug design, has demonstrated a crucial part for the discovery of new molecules in pharmaceutical design, drug metabolism, and medicinal chemistry (Adeniji et al. 2019). This approach had facilitated the improvement in the course of optimization of chemical structures with well-defined purposes (Adeniji et al. 2020c). Quantitative structure-activity relationship study and molecular docking are one of the computer-aided drug design approaches which had been broadly utilized in the design, improvement, and synthesis of first-hand drug (Adeniji et al. 2020a). QSAR investigation had shown to be an expedient technique for forecasting biological/inhibition activities, properties of any chemical compound by making use of an experimental data, and molecular descriptors. This idea is based on the correlation between the information derived from any chemical space or structural molecule illustrated by the descriptor and well-defined experimental data provided. Meanwhile, molecular docking technique helps to foresee the binding location and affinity of the existing interaction between the molecule (ligand) and the target, thereby providing an idea to design a prospective drug with better activity against the target (Adeniji et al. 2020a). Therefore, the study aimed to carry out computational investigation, virtual docking simulation of 1,2,4-triazole analogues, and in silico design of new proposed compounds against DNA gyrase.

## Methods

### Collection of dataset

Forty molecules comprising the analogues of 1,2,4-triazole reported as anti-tubercular agents that were used in this study were acquired from the literature (<https://patents.justia.com/patent/8865910>). The general structure of analogues of 1,2,4-triazole and the predicted and experimental activities of these compounds were presented in Fig. 1 and Table 1, respectively.

### Optimization and descriptor calculation

Optimization of the studied compounds so as to attain steady conformation was achieved with the aid of density

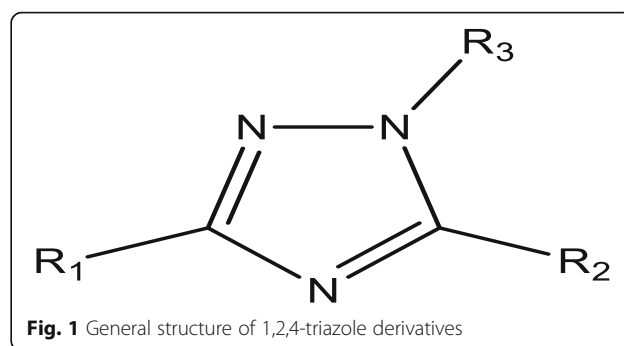


**Fig. 1** General structure of 1,2,4-triazole derivatives

**Table 1** Inhibitory compounds as anti-tubercular agents

S/N	Molecules	Experimental activity (pBA)	Predicted activity (pBA)	Residual	Leverage
1 <sup>a</sup>	1-benzyl-4-(((1-((1-benzyl-1H-1,2,3-triazol-4-yl)methyl)-3-(tert-butyl)-1H-1,2,4-triazol-5-yl)thio)methyl)-1H-1,2,3-triazole	5.7268	6.0896	-0.3628	0.1619
2	1-benzyl-4-(((1-((1-benzyl-1H-1,2,3-triazol-4-yl)methyl)-3-(4-nitrophenyl)-1H-1,2,4-triazol-5-yl)thio)methyl)-1H-1,2,3-triazole	5.5023	5.3625	0.1398	0.2423
3 <sup>a</sup>	1-benzyl-4-(((1-((1-benzyl-1H-1,2,3-triazol-4-yl)methyl)-3-(4-methoxyphenyl)-1H-1,2,4-triazol-5-yl)thio)methyl)-1H-1,2,3-triazole	6.007	6.3186	-0.3116	0.1304
4 <sup>a</sup>	1-benzyl-4-(((1-((1-benzyl-1H-1,2,3-triazol-4-yl)methyl)-3-(4-chlorophenyl)-1H-1,2,4-triazol-5-yl)thio)methyl)-1H-1,2,3-triazole	5.0064	5.5561	-0.5497	0.3033
5 <sup>a</sup>	3-(allylthio)-1H-1,2,4-triazole	5.7317	5.6841	0.0476	0.0303
6	1-benzyl-4-(((1-((1-benzyl-1H-1,2,3-triazol-4-yl)methyl)-5-(tert-butyl)-1H-1,2,4-triazol-3-yl)thio)methyl)-1H-1,2,3-triazole	5.6376	5.5557	0.0819	0.3826
7	1-benzyl-4-(((1-((1-benzyl-1H-1,2,3-triazol-4-yl)methyl)-5-(4-methoxyphenyl)-1H-1,2,4-triazol-3-yl)thio)methyl)-1H-1,2,3-triazole	4.7441	5.1002	-0.3561	0.3538
8	1-benzyl-4-(((1-((1-benzyl-1H-1,2,3-triazol-4-yl)methyl)-5-(4-chlorophenyl)-1H-1,2,4-triazol-3-yl)thio)methyl)-1H-1,2,3-triazole	6.1674	5.9575	0.2099	0.0601
9 <sup>a</sup>	1-benzyl-4-(((1-((1-benzyl-1H-1,2,3-triazol-4-yl)methyl)-1H-1,2,4-triazol-5-yl)thio)methyl)-1H-1,2,3-triazole	6.3713	6.9926	-0.6213	0.3184
10	1-benzyl-4-(((1-((1-benzyl-1H-1,2,3-triazol-4-yl)methyl)-3-methyl-1H-1,2,4-triazol-5-yl)thio)methyl)-1H-1,2,3-triazole	7.4134	7.2209	0.1925	0.0598
11	5-(4-nitrophenyl)-3-(prop-2-yn-1-ylsulfonyl)-1H-1,2,4-triazole	5.7441	6.3581	-0.614	0.0714
12	5-(4-methoxyphenyl)-3-(prop-2-yn-1-ylsulfonyl)-1H-1,2,4-triazole	5.9258	6.0358	-0.11	0.0424
13	5-(4-chlorophenyl)-3-(prop-2-yn-1-ylsulfonyl)-1H-1,2,4-triazole	7.5281	7.0701	0.458	0.0762
14	1-allyl-3-(tert-butyl)-5-(prop-2-yn-1-ylthio)-1H-1,2,4-triazole	6.3793	6.2871	0.0922	0.1938
15 <sup>a</sup>	1-allyl-5-(tert-butyl)-3-(prop-2-yn-1-ylthio)-1H-1,2,4-triazole	8.0615	7.5772	0.4843	0.0658
16	5-(allylthio)-3-methyl-1H-1,2,4-triazole	7.8807	7.7668	0.1139	0.0504
17	5-(allylthio)-3-(tert-butyl)-1H-1,2,4-triazole	6.4171	6.4769	-0.0598	0.1296
18	5-(allylthio)-3-(4-nitrophenyl)-1H-1,2,4-triazole	5.9471	6.443	-0.4959	0.0347
19	3-(allylthio)-5-(4-chlorophenyl)-1H-1,2,4-triazole	8.0899	7.7759	0.314	0.1757
20	3-(allylthio)-5-(4-methoxyphenyl)-1H-1,2,4-triazole	7.6397	7.7175	-0.0778	0.3321
21	1-allyl-3-(allylthio)-1H-1,2,4-triazole	6.3981	5.9875	0.4106	0.4076
22	1-allyl-3-(allylthio)-5-methyl-1H-1,2,4-triazole	5.8131	6.3817	-0.5686	0.2386
23	1-allyl-3-(allylthio)-5-(tert-butyl)-1H-1,2,4-triazole	6.2878	6.2104	0.0774	0.2302
24 <sup>a</sup>	1-allyl-3-(allylthio)-5-(4-nitrophenyl)-1H-1,2,4-triazole	8.0615	7.703	0.3585	0.2547
25	1-allyl-3-(allylthio)-5-(4-methoxyphenyl)-1H-1,2,4-triazole	7.366	6.8935	0.4725	0.3849
26	1-allyl-3-(allylthio)-5-(4-chlorophenyl)-1H-1,2,4-triazole	7.659	6.844	0.815	0.232
27 <sup>a</sup>	1-allyl-5-(allylthio)-1H-1,2,4-triazole	7.9432	7.7982	0.145	0.0307
28 <sup>a</sup>	1-allyl-5-(allylthio)-3-methyl-1H-1,2,4-triazole	7.9759	8.6181	-0.6422	0.4921
29 <sup>a</sup>	1-allyl-5-(allylthio)-3-(tert-butyl)-1H-1,2,4-triazole	5.2717	7.6208	-2.3491	0.3163
30	1-allyl-5-(allylthio)-3-(4-nitrophenyl)-1H-1,2,4-triazole	6.304	6.0214	0.2826	0.1944
31	1-allyl-5-(allylthio)-3-(4-methoxyphenyl)-1H-1,2,4-triazole	7.3233	7.1344	0.1889	0.4957
32	1-allyl-5-(allylthio)-3-(4-chlorophenyl)-1H-1,2,4-triazole	6.0097	6.995	-0.9853	0.0482
33 <sup>a</sup>	3-(prop-2-yn-1-ylsulfonyl)-1H-1,2,4-triazole	5.5994	5.735	-0.1356	0.095
34 <sup>a</sup>	5-methyl-3-(prop-2-yn-1-ylsulfonyl)-1H-1,2,4-triazole	4.9074	5.7514	-0.844	0.1017
35	5-(tert-butyl)-3-(prop-2-yn-1-ylsulfonyl)-1H-1,2,4-triazole	6.8568	6.9247	-0.0679	0.178
36	1-benzyl-4-(((3-methyl-1H-1,2,4-triazol-5-yl)thio)methyl)-1H-1,2,3-triazole	7.8456	7.1946	0.651	0.0981
37	4-(((1H-1,2,4-triazol-5-yl)thio)methyl)-1-benzyl-1H-1,2,3-triazole	7.3079	7.9753	-0.6674	0.0334

**Table 1** Inhibitory compounds as anti-tubercular agents (*Continued*)

S/N	Molecules	Experimental activity (pBA)	Predicted activity (pBA)	Residual	Leverage
38	1-benzyl-4-(((3-(tert-butyl)-1H-1,2,4-triazol-5-yl)thio)methyl)-1H-1,2,3-triazole	7.314	7.7043	-0.3903	0.7119
39	1-benzyl-4-(((1-((1-benzyl-1H-1,2,3-triazol-4-yl)methyl)-1H-1,2,4-triazol-3-yl)thio)methyl)-1H-1,2,3-triazole	6.8719	7.1271	-0.2552	0.2365
40	1-benzyl-4-(((1-((1-benzyl-1H-1,2,3-triazol-4-yl)methyl)-5-methyl-1H-1,2,4-triazol-3-yl)thio)methyl)-1H-1,2,3-triazole	7.9759	7.7716	0.2043	0.6105

Superscript "a" represents the test set. The calculated activity (pA) is generated using the QSAR model built in this study. The residual values are the difference between the observed activity (pA) and calculated activity (pA). Leverage value for each compound represents the diagonal element of the hat matrix which defines the applicability domain space of the each compound

functional theory [DFT (B3LYP/631G\*)] using Spartan 14 (Adeniji et al. 2019). Each optimized structure was imported into PaDEL Descriptor software which calculated about 1876 molecular descriptors. These descriptors provide relevant information on the potential hydrogen bonds of path length, potential electronic properties, hydrophobic, relative ionization, and steric which may sway the biological activity.

#### Pretreatment of calculated descriptors and splitting of dataset

All calculated descriptors were screened using a pretreatment 1.2 software so as to eliminate redundant and descriptors with less information in order to build an optimum model with high predictability (Adeniji et al. 2020c). Meanwhile, Kennard and Stone's algorithm method available in Data-division 1.2 software was employed to split the data into modeling dataset (training set) and validation dataset (test set) with a ratio of 7:3, i.e., 70 to 30%. Model construction was executed on the training set while the validity and confirmation were checked on the test set.

#### Construction of QSAR models and validation test

Construction of optimum model that could serve as a tool for predicting reported experimental biodata and also serve as a tool to design novel compound was developed using the genetic function approximation approach. This technique randomly selected combined descriptors that could give a good prediction of the dataset. To generate the model in linear equation form, the idea of multiple-linear regression was adopted to generate the multivariant equation which was executed in the Material Studio software version

8.0 and also to assess the internal validation of the built model.

#### Leverage measure (applicability domain)

Leverage ( $hi$ ) values for the dataset that made up the studied compound were calculated in order to define the chemical space (applicability domain) of the model built. Graphical interpretation of the leverage value for each of the compound plotted against their respective standardized residual is described as Williams' plot. The diagonal of the hat matrix element is termed the leverage calculated for both the training and test sets; meanwhile, the standardized residual is the validated residual estimated between predicted and reported experiment activities for both the training and test sets. The leverage ( $hi$ ) was calculated using Eq. 1 which was used to check for outlier compound at a defined space (applicability domain boundary) of  $\pm 3$  (Adeniji et al. 2020b):

$$hi = N_j (N^T N)^{-1} N_j^T \quad (1)$$

$N_j$  denotes the matrix of  $i$  for the modeling set (training data).  $N$  denotes the  $m \times d$  matrix for the training data, and  $N^T$  is the transpose of the training data ( $N$ ).  $N_j^T$  denotes the transpose matrix  $N_j$ . In order to evaluate for an influential molecule, the warning leverage  $h^*$  defined in Eq. 2 was calculated to define the limit boundary:

$$h^* = 3 \frac{(d+1)}{N} \quad (2)$$

where  $d$  and  $N$  denoted the number of descriptors and the number of training data (Adeniji et al. 2020b).

**Table 2** Name of the selected descriptors used in the QSAR model

S/NO	Descriptor symbols	Name of descriptor	Class
1	<b>MATS7s</b>	Moran autocorrelation – lag 7/weighted by I-state	2D
2	<b>SM1_DzZ</b>	Spectral moment of order 1 from Barysz matrix/weighted by atomic number	2D
4	<b>TDB3v</b>	3D topological distance-based autocorrelation – lag 3/weighted by van der Waals volumes	D
5	<b>RDF70v</b>	Radial distribution function – 070/weighted by relative van der Waals volumes	3D

**Table 3** Calculated descriptors for training set in the model

Compound ID	Descriptors				Predicted activity
	MATS7s	SM1_DzZ	TDB3v	RDF70v	
<b>Training set</b>					
2	0.0026	1.4821	658.7772	2.0498	4.9250
6	-0.3317	1.9107	633.2209	15.5345	5.0064
7	-0.0516	2.1607	685.7303	13.2508	5.7386
8	-0.1336	2.5578	696.3924	24.0959	4.7441
10	-0.2464	1.9107	661.5998	22.5805	6.1674
11	-0.0726	1.9107	633.9043	24.8431	7.4134
12	0.1240	2.5536	695.4821	28.0128	5.7441
13	-0.1179	2.1607	688.6992	26.4488	5.9258
14	-0.1765	2.5578	699.4567	26.6119	6.3793
16	0.0551	1.0536	621.0873	0.2906	6.1667
17	-0.1773	1.0536	572.3149	1.7741	6.4171
18	0.3859	1.6964	732.5999	3.7133	5.9413
19	0.0766	1.3036	712.3987	2.8412	7.6397
20	-0.1182	1.7006	746.2645	3.1697	8.0899
21	0.0020	1.0536	591.6153	1.2108	6.3981
22	0.1950	1.0536	616.2699	2.0915	5.8131
23	-0.2311	1.0536	582.2291	2.0369	6.2878
25	0.1290	1.3036	688.9992	2.9870	5.7268
26	0.0164	1.7006	712.3814	3.6128	7.3660
30	0.2273	1.6964	707.5776	4.1750	6.5267
31	0.0180	1.3036	693.4308	3.4526	5.7405
32	-0.0601	1.7006	717.2290	3.2901	5.6533
35	-0.8213	1.5536	621.1500	5.2505	7.3233
36	-0.1353	2.1964	773.1185	5.3930	6.0097
37	-0.2347	1.8036	754.5958	5.1746	6.0928
38	-0.2668	2.2006	789.7752	5.0883	8.0990
39	0.0350	1.0536	622.7128	4.6434	6.8568
40	0.2186	1.0536	686.1800	1.0517	7.3079
<b>Test set</b>					
1	0.1841	1.6964	703.6135	4.0508	6.0916
3	0.0008	1.0536	584.7233	4.7949	6.3205
4	-0.1670	1.4821	618.5815	7.5425	5.5581
5	-0.2527	1.9107	651.0893	13.7845	5.6861
9	-0.1673	1.0536	619.5964	1.9757	6.9946
15	-0.0020	1.0536	625.8344	4.9127	7.5792
24	-0.4581	1.0536	634.4842	1.9049	7.7050
27	-0.0327	1.0536	669.1703	1.2825	7.8002
28	-0.1381	1.0536	694.5662	3.1503	8.6201
29	-0.0090	0.4286	550.5198	0.3573	7.6228
33	-0.1718	1.9107	657.0710	14.0439	5.7370
34	-0.3329	2.5143	731.9698	5.0947	5.7534

Descriptor value generated for each compound for the purpose of reproducibility

### Assessment of Y-randomization test

Another criterion to be considered while establishing a built model is the Y-randomization test. This assessment is an external validation test which was achieved by random shuffling on the training data. (Adeniji et al. 2020a; Roy et al. 2011; Adeniji et al. 2020d). In order to create the multiple-linear regression model, descriptors, i.e., independent variables, which are the independent variables were kept untouched while the biological activities, i.e., dependent variable, were shuffled. To establish that the created model is not accidentally obtained, the  $R^2$  and  $Q^2$  values for the built model must be relatively low for many trials. More also, the Y-randomization coefficient ( $cR_p^2$ ) presented in Eq. 3 must be  $\geq 0.5$  so as to affirm that the model is robust:

$$cR_p^2 = R \times [R^2 - (R_r)^2]^2 \quad (3)$$

$R_r$  is the average of  $R$  of random models, and  $R$  is the correlation coefficient (Adeniji et al. 2020d; Tropsha et al. 2003).

### Verification and confirmation of the built model

The constructed model was subjected to various statistical tools to verify the potency of the model. Moreover, the internal and external threshold values have been laid to ascertain and affirm any kind of built model for validation as reported in Table 6 (Adeniji et al. 2020a; Roy et al. 2011; Adeniji et al. 2020d; Tropsha et al. 2003; Adeniji et al. 2018). Therefore, both the internal and external tests reported in this work were compared and verified with the generally accepted threshold value to ascertain the potency and the robustness of the built model.

### Molecular docking procedure

Receptor-ligand docking interaction was carried out to know the binding affinity and to ascertain the possible ligand binding sites. The docking simulations were achieved using the AutoDock4.2 incorporated in the PyRx software. The targeted enzyme (DNA gyrase) in the form of crystal structure with PDB code 31FZ was

**Table 4** Pearson's correlation coefficient for the descriptor used in the QSAR model

	MATS7s	SM1_DzZ	TDB3v	RDF70v
<b>MATS7s</b>	1			
<b>SM1_DzZ</b>	-0.4244	1		
<b>TDB3v</b>	0.0743	0.1344	1	
<b>RDF70v</b>	-0.6903	0.0675	0.0534	1

Pearson's correlation coefficient to evaluate the multicollinearity between each descriptor

**Table 5** Statistical parameters that influence the model

Descriptors	Regression coefficient	Mean effect (ME)	p value (confidence interval)	VIF	Standard error
MATS7s	- 1.2762	- 0.2213	1.57E-07	2.7392	2.10E-08
SM1_DzZ	- 2.7874	- 0.9015	4.69E-05	3.8417	3.93E-06
TDB3v	0.2107	3.7301	3.91E-09	3.4016	3.02E-07
RDF70v	0.1488	1.0381	6.45E-05	4.4398	5.23E-06

Statistical consideration to evaluate the strength and magnitude of each descriptors, inter-existence between the descriptors and computational error

**Table 6** Validation parameters for each model using multilinear regression (MLR)

S/NO	Validation parameters	Formula	Threshold	Model
<b>Internal validation</b>				
1	Friedman lack of fit (LOF)	$\frac{SEE}{(1 - \frac{w+q \times l}{N})^2}$	Significantly low	0.1802
2	R-squared	$1 - \left[ \frac{\sum (Y_{obs} - Y_{pred})^2}{\sum (Y_{obs} - \bar{Y}_{training})^2} \right]$	$R^2 > 0.6$	0.7759
3	Adjusted R-squared	$\frac{R^2 - P(N-1)}{N-p+1}$	$R_{adj}^2 > 0.6$	0.7381
4	Cross-validated R-squared ( $Q_{cv}^2$ )	$1 - \left[ \frac{\sum (Y_{pred} - Y_{obs})^2}{\sum (Y_{obs} - \bar{Y}_{training})^2} \right]$	$Q^2 > 0.6$	0.6954
5	Significant regression			Yes
6	Significance-of-regression F value			13.42
7	Critical SOR F value (95%)	$\frac{\sum (Y_{pred} - Y_{obs})^2}{p} / \frac{\sum (Y_{pred} - Y_{obs})^2}{N-p-1}$	$F_{(test)} > 2.09$	2.7294
8	Replicate points			0
9	Computed observed error			0
10	Min expt. error for non-significant LOF (95%)			0.4120
<b>Model randomization</b>				
11	Average of the correlation coefficient for randomized data ( $\bar{R}_r$ )		$\bar{R} < 0.5$	0.3642
12	Average of determination coefficient for randomized data ( $\bar{R}_r^2$ )		$\bar{R}_r^2 < 0.5$	0.1823
13	Average of leave one out cross-validated determination coefficient for randomized data ( $\bar{Q}_r^2$ )		$\bar{Q}_r^2 < 0.5$	0.3915
14	Coefficient for Y-randomization ( $cR_p^2$ )	$R^2 \times (1 - \sqrt{ R^2 - \bar{R}_r^2 })$	$cR_p^2 > 0.6$	0.9229
<b>External validation</b>				
15	$ r_0^2 - r_o'^2 $		< 0.3	0.1591
16	$\frac{r^2 - r_0^2}{r^2}$		< 0.1	0.0023
17	$\frac{r^2 - r_o'^2}{r^2}$		< 0.1	0.0136
18	$R_{test}^2$	$R_{test}^2 = 1 - \frac{\sum (Y_{pred_{test}} - Y_{obs_{test}})^2}{\sum (Y_{pred_{test}} - \bar{Y}_{training})^2}$	> 0.6	0.6550

SEE is the standard error of estimation, w is the total number of terms present in the built model except the constant term, j is the number of descriptors confined in the built model, q is a user-defined factor, and N is the number of compounds of training set.  $Y_{obs}$ ,  $\bar{Y}_{training}$ , and  $Y_{pred}$  are the observed activity, the mean observed activity of the training compounds, and the predicted activity, respectively.  $r^2$  is the correlation coefficients of the plot of observed activity against predicted activity values,  $r_o'^2$  is the correlation coefficients of the plot of observed activity against predicted activity values at zero intercept, and  $r_0^2$  is the correlation coefficients of the plot of predicted activity against observed activity at zero intercept (Adeniji et al. 2020a; Roy et al. 2011; Adeniji et al. 2020d)

retrieved from a protein data bank (Piton et al. 2010; Piton et al. n.d.). With the Discovery Studio Visualizer software, all forms of solvent molecules, ligands, and cofactors imported with the enzyme were removed in order to achieve good binding interactions between the enzyme (protein) and the ligands (molecules). Thereafter, the enzyme protein was saved in PDB format which is recognized by the PyRx software and transformed as macromolecule (Adeniji et al. 2020a; Adeniji et al. 2018). Optimum conformation of the ligands (1,2,4-triazole derivatives) at minimum energy to enhance efficient binding interaction with the enzyme was achieved using Spartan 14 software as an optimized tool utilizing density functional theory [DFT (B3LYP/631G\*)]. Thereafter, all the ligands optimized were saved as PDB format which is also recognized by the PyRx software and transformed as micromolecules (Adeniji et al. 2020a; Adeniji et al. 2018). In the PyRx software, the docking interaction between the targeted enzyme and the protein was then computed to evaluate the binding affinities while the interaction types such as hydrogen bonding, electrostatic interaction, and hydrophobic interaction were visualized and analyzed using the Discovery Studio Visualizer 16 software (Adeniji et al. 2018; Ibrahim et al. 2020).

#### Procedure for the in silico design of novel triazole derivatives

Substitution, elimination, and addition techniques were employed to design some proposed anti-tubercular agents with enhanced activities via modification of the template structure (compound 19) using the approach of ligand-based design (Adeniji et al. 2020a; Adeniji et al. 2020b). The template was selected as the reference compound and backbone to design new promising compounds due to its prominent activity values found within the applicability domain phase. The discovery of the new compounds was successfully achieved based on the information derived for the computed mean effect on the descriptor with high influence on the biological activities.

## Results

### Proposed QSAR model

$$\text{pBA} = -1.276219502 \times \text{MATS7s} - 2.787371275 \times \text{SM1\_DzZ} + 0.020733853 \times \text{TDB3v} + 0.148823521 \times \text{RDF70v} + 1.546675296$$

## Discussion

Dataset comprises 1,2,4-triazole, and its analogue against *M. tuberculosis* was successfully split into 28

modeling datasets (training set) and 12 validation datasets (test set) with the algorithm laid by Kennard and Stone (Adeniji et al. 2020d). The 28 training set data was used to construct the genetic functional algorithm using the multilinear regression technique as a model equation.

The analysis of the derived genetic functional algorithm model explores the physicochemical and structural influence of the studied compounds with their respective anti-tubercular activities. The derived model was established with geometrical and topological descriptors: MATS7s, SM1\_DzZ, TDB3v, and RDF70v which influenced the model with relevant information and contribution as presented in Table 2. Meanwhile, all the calculated descriptors for the whole compounds for the purpose of validity and reproducibility are reported in Table 3. These descriptors were identified and correlated with anti-tubercular activity values.

Pearson's correlation statistics and variance inflation factor (VIF) were utilized to validate the descriptors in the proposed model (Adeniji et al. 2020b; Adeniji et al. 2020c; Roy et al. 2011; Adeniji et al. 2020d). Pearson's correlation statistics investigated between each descriptor were all  $\leq \pm 0.8$  as presented in Table 4 which signifies that no multicollinearity was found between each pair of descriptors. Interestingly, all the calculated values for the VIF reported in Table 5 are less than 10 which implies there is no inter-correlation existence for each descriptor. However, if the reported VIF value is  $> 10$ , this shows that the proposed model is likely unstable;

**Table 7** Y-randomization parameters test for model 1

Model	<i>R</i>	<i>R</i> <sup>2</sup>	<i>Q</i> <sup>2</sup>
Original	1	1	1
Random 1	0.5799	0.3363	-0.1498
Random 2	0.3665	0.1344	-0.4056
Random 3	0.3999	0.1599	-0.3927
Random 4	0.4189	0.1754	-0.3763
Random 5	0.1595	0.0254	-0.5045
Random 6	0.5494	0.3018	-0.1199
Random 7	0.2301	0.0530	-0.5541
Random 8	0.3366	0.1133	-0.4290
Random 9	0.3660	0.1340	-0.2959
Random 10	0.4405	0.1940	-0.2196
Random model parameters			
Average <i>r</i>	0.3642		
Average <i>r</i> <sup>2</sup>	0.1823		
Average <i>Q</i> <sup>2</sup>	-0.3915		
cRp <sup>2</sup>	0.9229		

Y-randomization test to ascertain the robustness of the model

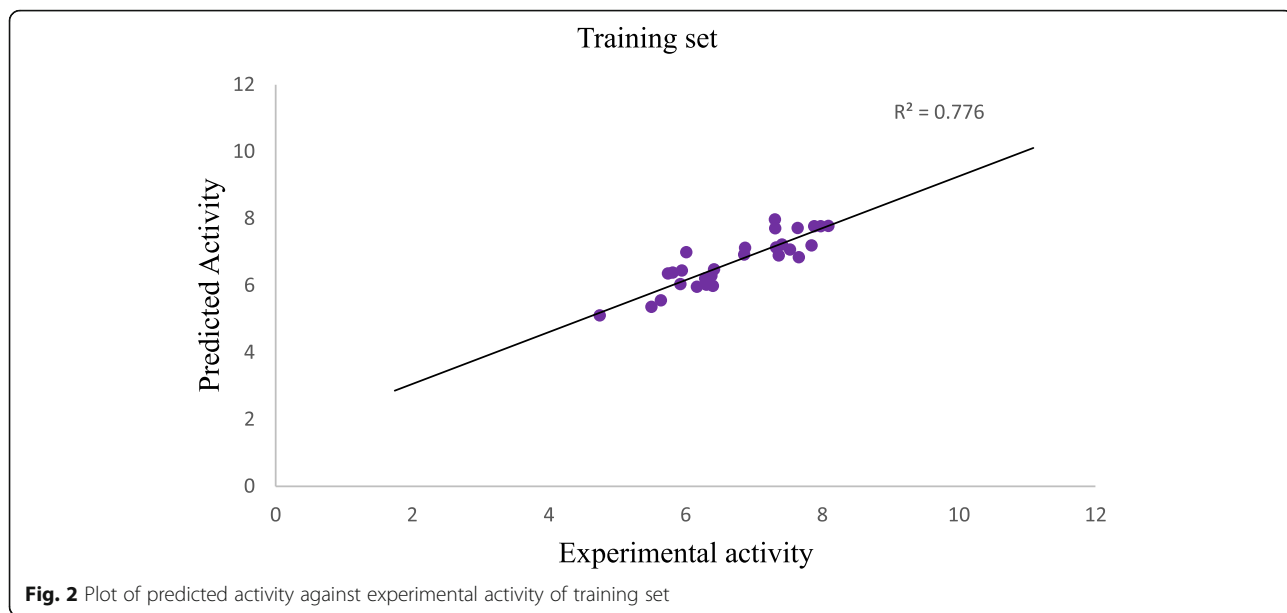


**Fig. 2** Plot of predicted activity against experimental activity of training set

therefore, the model needs to be rechecked (Adeniji et al. 2020a; Adeniji et al. 2020b; Adeniji et al. 2020c). Meanwhile, the results of the VIF are in full agreement with Pearson’s correlation statistics.

More also, another statistical parameter, i.e., one way analysis of variance (ANOVA), was computed to evaluate the significant correlation between the anti-tubercular activities and the descriptors at 95% confidence level. The probability values reported in Table 5

are found to be ( $p < 0.05$ ) for each of the descriptors. This signifies that the null hypothesis suggesting no correlation between anti-tubercular activities and the descriptors in the proposed model is annulled. Thus, the alternative hypothesis proposing a significant correlation between the anti-tubercular activities and the descriptor is accepted (Adeniji et al. 2020d).

The relative direction, importance, and contribution of each descriptor in the proposed model were computed

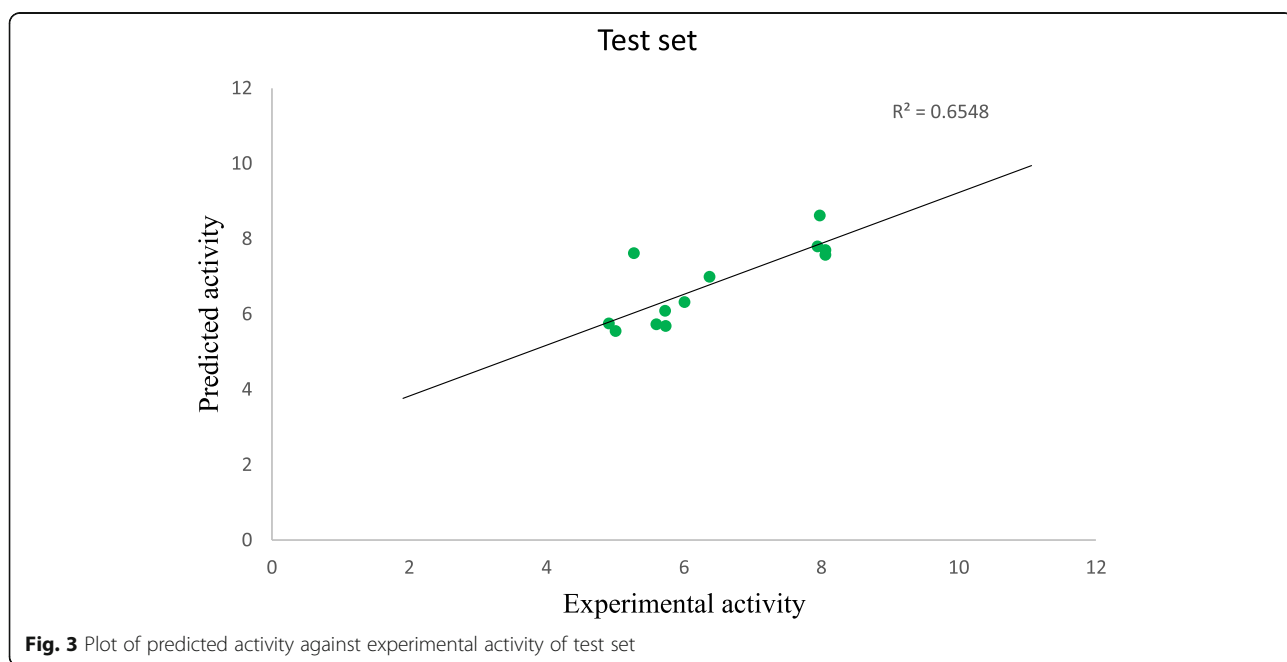


**Fig. 3** Plot of predicted activity against experimental activity of test set



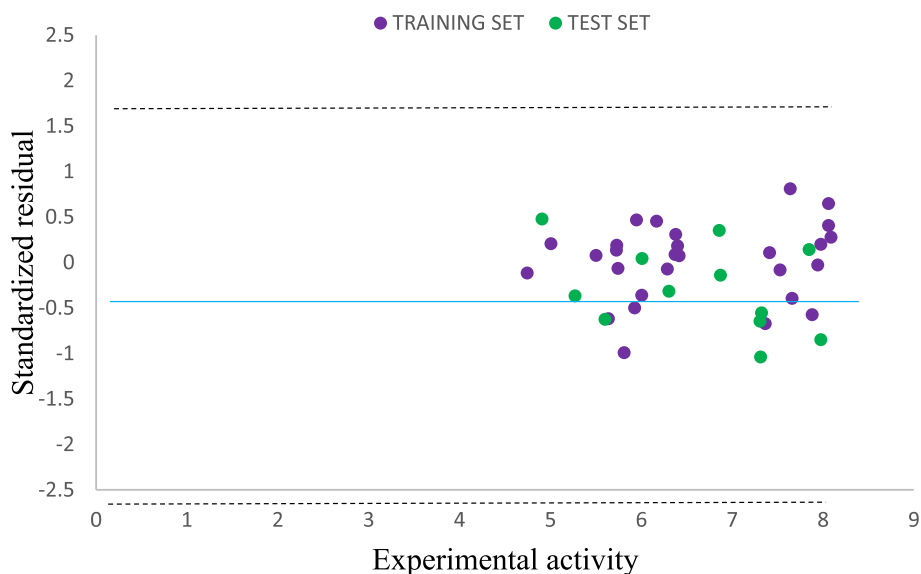


**Fig. 4** Plot of standardized residual activity versus experimental activity

using the mean effect (ME) approach as reported in Table 5. The value of the mean effect calculated for each descriptor in a model suggests the contribution that each descriptors plays in the model while the sign signifies the direction at which the descriptor influences the anti-tubercular activities (Adeniji et al. 2020b; Adeniji et al. 2020d).

The proposed model was validated internally by squared correlation coefficient ( $R^2 = 0.7759$ ), adjusted

squared correlation coefficient ( $R_{adj}^2 = 0.7381$ ), and leave one out cross-validation squared correlation coefficient ( $Q^2 = 0.6954$ ) values (Table 6). Meanwhile, the robustness and fitness of the constructed models were ascertained by  $Y$ -randomization coefficient ( $cR_p^2 = 0.9229$ ) as reported in Table 7 to strongly affirm that the proposed model is not derived by chance. Externally, the proposed model was also cross-validated with significant

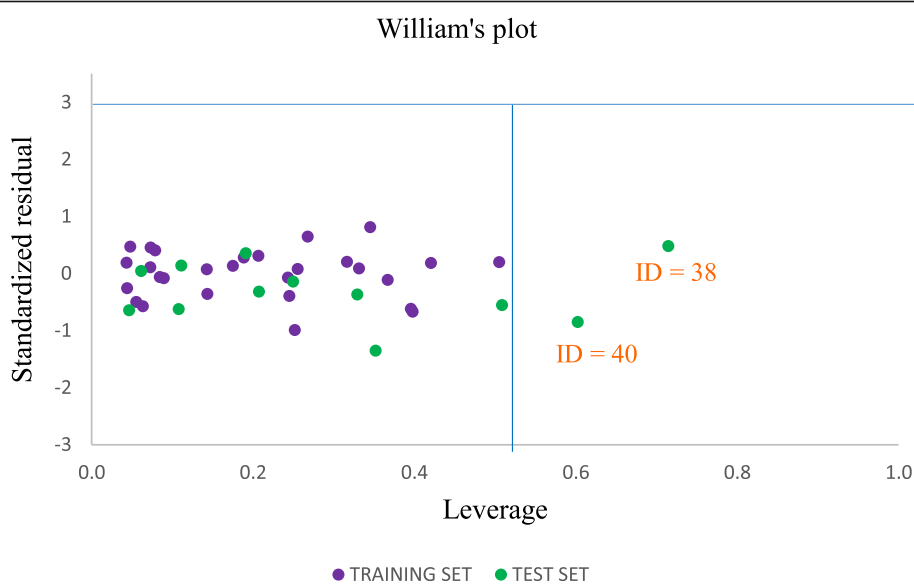


**Fig. 5** The Williams plot of the standardized residuals versus the leverage value. The Williams plot to determine the influential and outlier molecule and defined boundary  $\pm 3$  and warning leverage  $h^* = 0.64$

**Table 8** Docking analysis between triazole analogue and the target (DNA gyrase)

Ligand	Binding affinity (BA), kcal/mol	Hydrogen bond		Hydrophobic interaction
		Amino acid	Bond length (Å°)	Amino acid
1	- 6.09	ASN74	1.3454	PRO134, VAL78, LA167, ALA233
2	- 6.49	GLN385	1.6445	VAL83, VAL83, LEU76, TRP182
3	- 6.09	LEU103 TRP182	2.3421 3.0328	ALA233, PRO346, ALA167
4	- 5.89	ASN74	2.7656	ALA167, LEU164, VAL83
5	- 7.69	GLN383	2.8102	PHE338, CYS345, VAL83
6	- 5.99	ALA1 23	1.2233	PHE248, VAL228, CYS143, LEU176
7	- 3.99	-	-	TRP182, ALA167, VAL78, SER247, CYS145
8	- 7.49	ALA167	2.4332	CYS221, TRP182, ALA212, PRO165
9	- 7.59	GLN385	1.3443	ALA143, TRP182, PHE168
10	- 12.29	THR77 GLN385	2.4554 2.4332	LEU164, VAL78, VAL228, ALA236
11	- 4.09	-	-	PHE243, ALA167
12	- 6.19	VAL112	1.3452	ALA203, PHE130, VAL78
13	- 12.69	-	-	PHE128, VAL78, PRO232, VAL128, SER237
14	- 6.39	THR87	1.4234	ALA237, TRP123, LEU154, VAL228
15	- 9.439	THR78	1.2433	ALA167, TRP122, LEU184, VAL228, VAL73
16	- 13.69	ASP110 PHE109 ALA111	2.3503 2.1532 2.6856	TYR113, PRO112
17	- 8.69	GLN385 CYS345	2.7332 2.4333	VAL78, ALA233, TRP182, VAL78
18	- 7.69	GLN385	2.5433	PRO285, PHE168, ALA167, VAL83, PRO285, VAL83
19	- 17.79	GLN101 TRP103 SER118 ASP122 ASP122	2.29648 2.28554 2.43913 2.99768 2.22618	TRP103
20	- 14.59	VAL78 ALA233 LEU76	2.1322 2.4876 2.4517	SER237, THR238, PHE168, PRO285, VAL78, ALA167
21	- 8.59	ASN78 ASP232	3.0175 2.2831	LEU207, VAL228, LEU73, VAL78, PRO245
22	- 6.19	THR77	2.4532	PHE168, TRP182, TRP182, PHE168, VAL78, ALA167
23	- 8.09	GLN385 SER237	2.1265 2.2453	PRO285, PHE338, CYS345, VAL78, ALA233
24	- 14.09	TRP182	1.7232	VAL82, PRO285, VAL78, VAL78, ALA167, PRO285
25	- 7.89	ASP282 LYS136 GLN385	2.1238 2.1433 2.2334	LEU103, VAL78, TRP182, ALA167, PRO285
26	- 14.79	GLN105 ALA167 VAL82	2.2339 2.2344 2.5753	LYS173, ALA128, PHE168, TRP182, PHE230, ALA111, PRO112, VAL82, VAL78
27	- 9.19	ASP78 GLN385	3.3648 2.4850	PRO346, ALA167, PHE168, TRP182, CYS345, ALA233
28	- 10.59	VAL77	2.4322	TRP182, ALA167, TRP182, PRO285, VAL27, PRO34
29	- 6.79	ASN74	3.4567	VAL99, PHE280, VAL142
30	- 7.59	GLN385	2.17739	VAL78, ALA233, LEU161, PHE168, TRP18

**Table 8** Docking analysis between triazole analogue and the target (DNA gyrase) (Continued)

Ligand	Binding affinity (BA), kcal/mol	Hydrogen bond		Hydrophobic interaction
		Amino acid	Bond length (Å)	Amino acid
31	- 14.29	LEU103	2.2281	PHE215, LEU207, MET66, VAL78, ALA147, PRO94
		GLN385	2.0343	
		CYS170	2.1732	
32	- 7.79	VAL95	2.6433	LEU217, TYR113, PRO112, VAL78
33	- 6.19	GLN105	2.5433	ALA137, VAL122, TRP182, PHE220
		ARG72	2.1843	
34	- 4.09	THR77	2.1123	PHE168, VAL78
		GLN385	2.6234	
		ALA167	2.6012	
		GLN385	2.1922	
		ALA167	2.6302	
35	- 8.19	THR77	2.1423	GLY232, VAL228, PHE168, TRP182, LYS175, ALA233
		ALA167	2.3432	
		GLN385	2.134	
36	- 14.59	PHE164	2.2211	PHE168, TRP182, PRO169, LYS136, VAL78, ALA167
		CYS134	2.211	
		GLY232	2.3732	
37	- 9.23	ARG165	1.99395	ALA167, PHE185, VAL228, CYS134, ASN74
		GLN385	2.3433	
		ARG386	2.4551	
38	- 6.89	THR65	1.43511	CYS170, ALA233, GLN385
39	- 8.29	GLN385	1.322	ARG165, GLN385, CYS234, VAL167, GLN385
40	- 15.69	-	-	LEU103, GLY96, PHE205, ARG101, LEU207
Isoniazid	- 14.6	SER279	2.29943	PHE338, CYS345
		ALA337	2.52954, 2.24657	

predictive squared correlation coefficient ( $R^2_{\text{Pred}} = 0.6550$ ) which all met the threshold requirement for accepting any proposed model reported in Table 6.

The proposed QSAR model and the findings gotten in this study were compared with the recent model established in the literature as presented below (Adeniji et al. 2020b):

$$\begin{aligned} \text{pBA} = & -3.927401745(\text{MATS2s}) \\ & + 4.730973152(\text{nHBint3}) \\ & + 1.1035920582(\text{maxtsC}) \\ & + 0.310934301(\text{TDB9u}) \\ & - 0.791306892(\text{RDF90i}) \\ & - 4.281096493(\text{RDF110s}) \\ & + 8.840916286 \end{aligned}$$

$$\begin{aligned} N_{\text{train}} = 35, N_{\text{test}} = 15, (R^2 = 0.9368), \\ (R^2_{\text{adj}} = 0.8960) (Q^2 = 0.8550) \\ (cR^2_p = 0.6849) (R^2_{\text{Pred}} = 0.7925) \end{aligned}$$

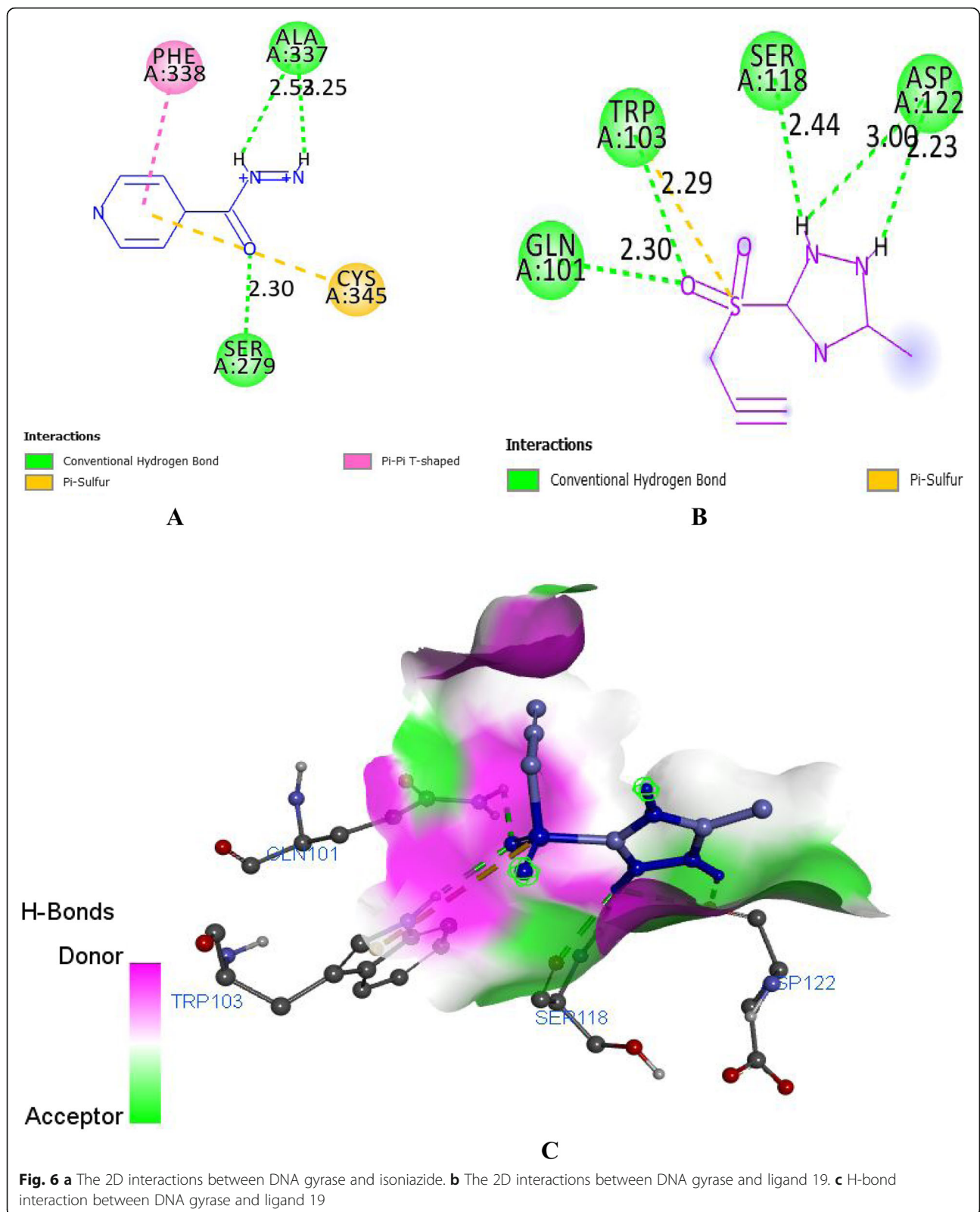
The validation factors stated in the literature and compared with those reported in this study were all in full

agreement with the threshold criteria reported in Table 6 which really implies and affirms that the proposed model is robust and fitted.

In addition, the coefficient ( $R^2$ ) values of 0.7659 and 0.6550 presented Figs. 2 and 3 for training and test sets also support the degree of correlation between the predicted anti-tubercular activities in this work and the reported experimental anti-tubercular activities in the literature. More also, the correlation coefficient ( $R^2$ ) values also fall with the minimum threshold value reported in Table 6 for any accepted proposed QSAR model.

The residual plot shown in Fig. 4 suggests that this model can be used for the prediction of the anti-tubercular activity values for new compound since all the standardized residual values for training and test sets fall within the distinct boundary of  $\pm 2$  on the vertical axis, i.e., standard residual axis. Moreover, the low residual value computed ascertains no inaccuracy and no computational incompetency in the model prediction (Adeniji et al. 2020c; Adeniji et al. 2020d).

Applicability domain (AD) ensures that the proposed model is vividly used only to predict compounds similar



in terms of distance measure, i.e., leverage  $h$  (Adeniji et al. 2020a; Adeniji et al. 2020b; Adeniji et al. 2020c; Roy et al. 2011; Adeniji et al. 2020d; Tropsha et al. 2003). AD for the proposed model using the Williams plots is presented in Fig. 5 which gives a graphical discovery of both influential compounds and outliers. The leverage measure is used to detect the outlier while warning leverage  $h^*$  is used to detect the influential compound. In Fig. 5, all the compounds appeared to fall within the defined leverage measure of  $\pm 3$ . Hence, no compound is said to be an outlier. However, compounds 38 and 40 are influential molecules since their computed leverage values exceed the warning leverage of  $h^* = 0.54$ .

### Molecular docking analysis

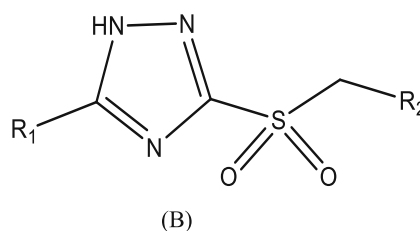
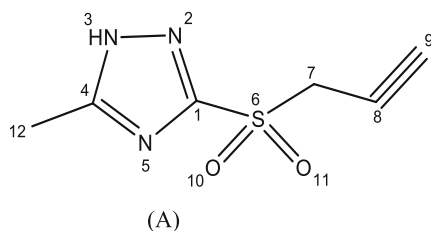
Analysis of docking interactions of the studied compounds with the protein target (DNA gyrase) is presented in Table 8. Interaction binding affinities between the protein binding pocket and the ligands range from  $-4.09$  to  $-17.79$  kcal/mol as shown in Table 8. Meanwhile, when the binding affinity of the conventional drugs, i.e., isoniazide ( $-14.6$  kcal mol $^{-1}$ ), was compared with the binding affinities of the studied compounds, it was observed that compound 19 among the 1,2,4-triazole analogues has a binding affinity of  $-17.79$  kcal mol $^{-1}$  greater than conventional drugs and other derivatives. Thus, ligand (compound 19) was visualized and evaluated using Discovery Studio Visualizer to ascertain its binding and interaction type. The 2-dimension interaction of ligand 19 with the protein target site is shown in Fig. 6. Five conventional hydrogen bonds (2.29648, 2.28554, 2.43913, 2.99768, and 2.22618°A) were bonded with GLN101, TRP103, SER118, ASP122, and ASP122. Two hydrogen bonds were observed with the S=O of the ligand as an H-acceptor and linked with GLN101 and TRP103 of the protein active site while three hydrogen bonds were observed with the N-H group as an H-donor with SER118, ASP122, and ASP122 of the protein active site as reported in Fig. 8. Increase in the number of hydrogen bonding in ligand 19 compared to three conventional

hydrogen bonds in isoniazide, i.e., 2.3001, 2.5301, and 2.2161°A, with ALA337, ALA337, and SER279 as presented in Fig. 8 accounts for the potency of ligand 19 over the commended drug.

### Computational design of novel anti-tubercular agents

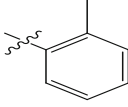
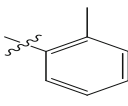
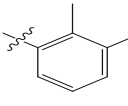
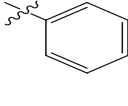
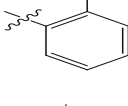
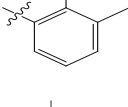
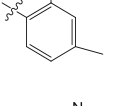
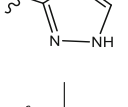
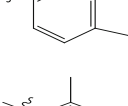
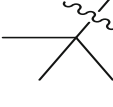
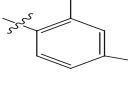
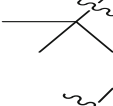
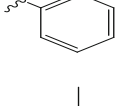
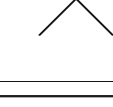
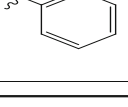
Substitution, elimination, and addition techniques were employed to design some novel anti-tubercular agents with enhanced activities via modification of the template structure (compound 19) presented in Fig. 7 using the approach of ligand-based design (Adeniji et al. 2020a; Adeniji et al. 2020b). The template was selected as the reference compound and backbone to design new promising compounds due to its prominent activity values found within the applicability domain phase reported in Fig. 5. The discovery of the new compounds was successfully achieved based on the information derived for the computed mean effect on the descriptor: TDB3v and RDF70v with high influence on the biological activities of the studied compounds and substitution and deletion which was simply made on the position of acetylene and 1H-1,2,4-triazole moiety at positions 8 and 12 seen in Fig. 7. Based on the approach, twelve prominent compounds with improved anti-tubercular activities were successfully designed by substituting and eliminating the alkyl group, H atom, methoxy group, and 1H-1,2,4-triazole at positions 8 and 12 of the reference presented in Table 9. To ascertain and affirm the reliability of the designed compounds, leverage value was computed for all the designed compounds. Interestingly, all the computed leverage values for the designed compounds appeared to fall the warning leverage ( $h^* = 0.64$ ) in Fig. 5. Meanwhile, compound 19h was observed with high activity among the designed compounds. This was as a result of the alkyl group (CH $_3$ ) substituted at position 12 and 1H-1,2,4-triazole substituted at position 8 of the reference template acting as electron donating substituents via positive inductive effect (+I), thereby increasing the electron density and making the pharmacophore of compound 19h more basic compared to other designed compounds.

### Discussion on designed compounds



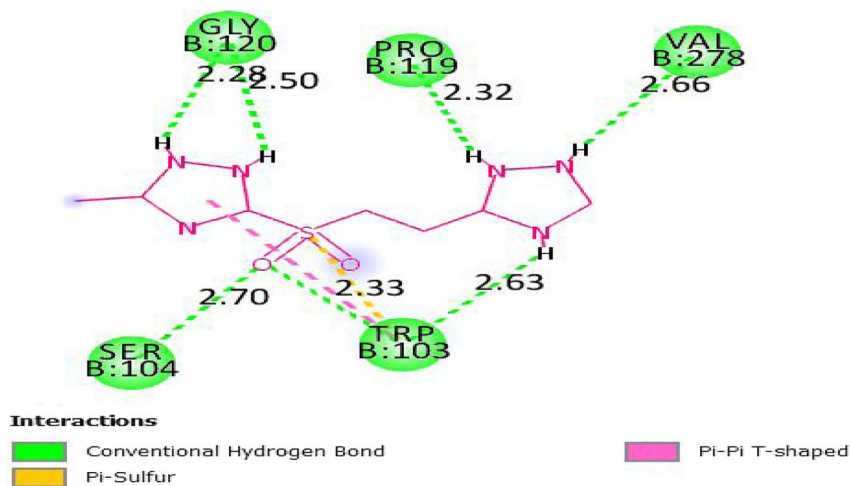
**Fig. 7 a** The lead compound (19). **b** The general formula of the lead compound (19) as a design template

**Table 9** Generated descriptors and predicted activities for the designed compounds

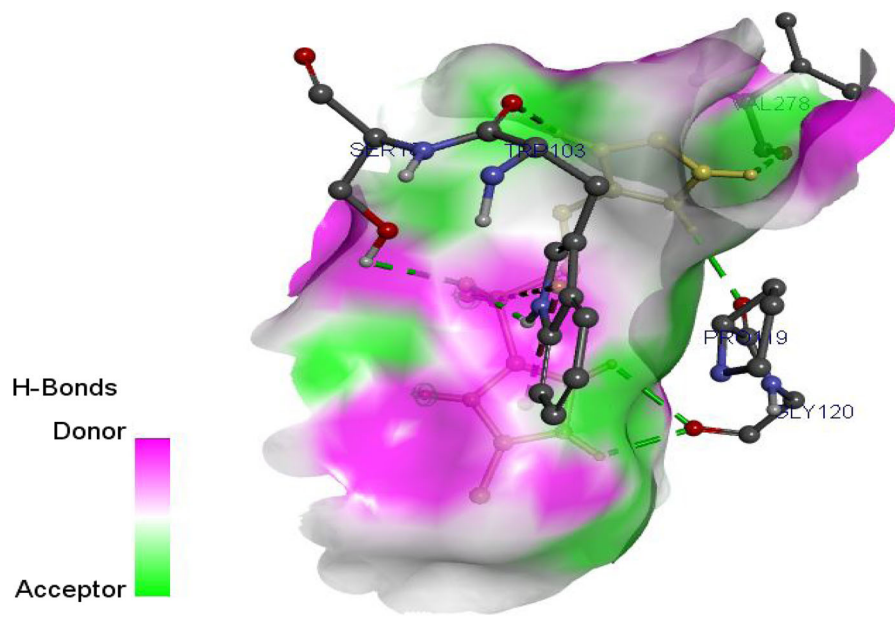
Compound ID	R <sub>1</sub>	R <sub>2</sub>	MATS 7s	SM1_D zZ	TDB3 v	RDF7 0v	Predicted Activity (pBA)	Leverage
19a	H		0.2629	1.9681	671.547	8.3931	6.9885	0.3542
19b	CH <sub>3</sub>		0.2107	1.9681	664.297	10.6445	7.147	0.3107
19c	OCH <sub>3</sub>		0.3635	1.5395	637.247	3.8344	6.97	0.4313
19d	CH <sub>3</sub> CH <sub>2</sub>		0.5103	1.5395	661.467	3.5793	7.021	0.4583
19e	CH <sub>3</sub> CH <sub>2</sub>		0.2908	1.5395	634.607	3.8695	6.3916	0.4598
19f	CH <sub>3</sub> CH <sub>2</sub>		-0.3783	1.3681	677.867	2.928	7.7183	0.2523
19g	CH <sub>3</sub>		-0.32411	1.7895	625.447	2.0971	6.021	0.541
19h	CH <sub>3</sub>		-0.12799	1.5395	645.007	15.2253	8.5032	0.1517
19i	H		-0.1572	2.2181	647.317	13.8481	6.7968	0.2561
19j			-0.1928	1.6152	663.577	9.8302	8.2649	0.3296
19k			-0.2662	1.5395	629.697	6.6262	7.1397	0.412
19l			-0.2651	1.5395	648.307	8.1964	7.338	0.521

**Table 10** Docking analysis between designed compound 19h and the target (DNA gyrase)

Ligand	Binding affinity (BA), kcal/mol	Hydrogen bond		Hydrophobic interaction	
		Amino acid	Bond length (Å)	Bond length (Å)	Amino acid
19h	-21.6	TRP103	2.32531		TRP103
		SER104	2.69785		
		GLY120	2.50087		
		GLY120	2.27506		
		PRO119	2.31546		
		VAL278	2.66424		
		TRP103	2.63031		

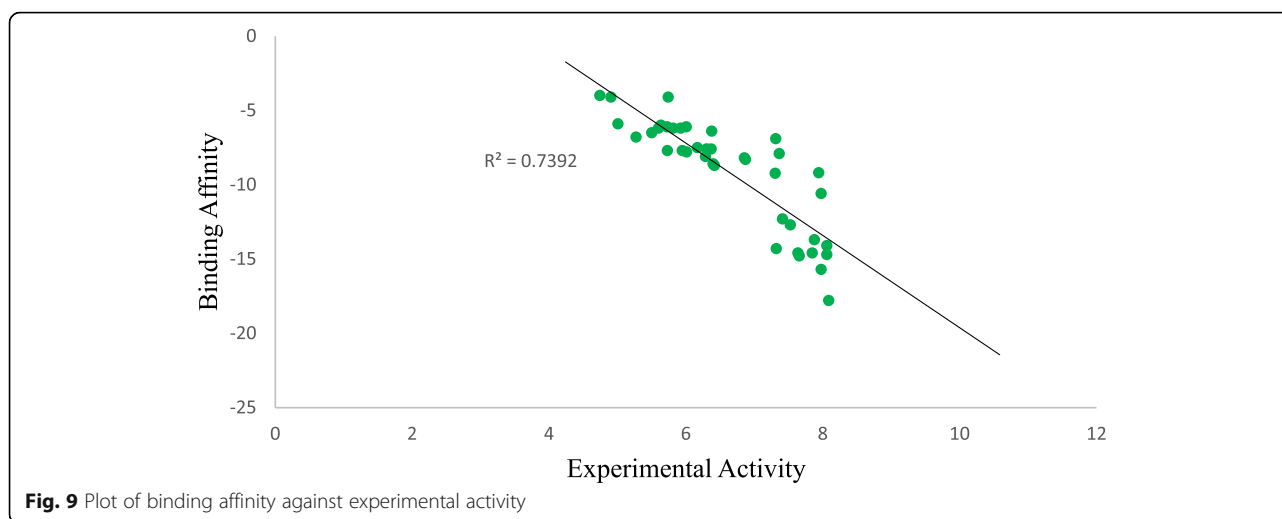


A



B

**Fig. 8 a** The 2D interactions between DNA gyrase and designed ligand 19h. **b** The H-bond interaction between DNA gyrase and designed ligand 19h



### Validation of designed compound 19h via molecular docking

Designed compound 19h was docked with the protein target (DNA gyrase) in order to confirm its potency with the binding site of the target. The target formed  $-21.6$  kcal/mol binding affinity with the ligand (compound 19h) as stated in Table 10 which appeared to be higher than the template (compound 19) binding affinity ( $-17.79$  kcal/mol) stated in Table 8. Ligand 19h formed seven conventional hydrogen bonds with targeted protein. The triazole “N-H group” acting as an H-bond donor provides contribution of five hydrogen bond linkages: two H-bonds with GLY120, one H-bond with PRO B:119, single H-bond with VAL278, and one H-bond with TRP103. More also, the triazole “S=O” acting as an H-bond acceptor provides meaningfully two H-bond bonds with TRP103 and SER104 as presented in Fig. 8. The increase in the number of hydrogen bonds in the receptor-ligand complex gives reasonable explanation why the binding affinity of designed compound 19h is higher than its reference template structure (compound 19) since more hydrogen bonds are observed in the designed compounds (Adeniji et al. 2020a; Adeniji et al. 2020b). Finally, the correlation between the QSAR studies and molecular docking is presented in Fig. 9. It is seen that the anti-tubercular activity of each molecule that made up the dataset coincides with the binding affinity with significant correlation of  $R^2 = 0.7206$ . Therefore, this signifies that there is relationship between the QSAR and molecular docking results at  $p < 0.05$ .

### Conclusion

Combined in silico and theoretical approach was successfully applied to derive a proposed QSAR model capable of predicting the activities of 1,2,4-triazole and its

analogue against *M. tuberculosis*. This model serves as a prominent tool for structural insight to design new hypothetical anti-tubercular compounds against multiple strain *M. tuberculosis*. Meanwhile, the reliability, significance, fitness, and robustness of the model have been fully established via internal and external assessments and validated molecular descriptors: MATS7s, SM1\_DzZ, TDB3v, and RDF70v that influence the anti-tubercular activities. Analysis of leverage measure also showed that the proposed model has a high predictability rate to predict all the anti-tubercular compounds that fall within its applicability domain space. In addition, docking studies showed that compound 19 has noticeable binding affinities from  $-17.79$  kcal/mol. Hence, it served as a structural template and insight to design twelve novel hypothetical agents with more competent activities. Meanwhile, compound 19h was observed with high activity among the designed compounds with a prominent binding affinity of  $-21.6$  kcal/mol. Therefore, in vivo, in vitro screening and pharmacokinetic properties should be carried out in order to determine the toxicity of the designed compounds.

### Acknowledgements

None

### Authors' contributions

SE, DE, MA, and OB did the conception and design of the work. SE, MA, and OB did the acquisition and analysis of the data. SE, DE, and MA interpreted the data. SE drafted the manuscript. SE substantively revised the manuscript. All authors read and approved the final manuscript.

### Funding

None

### Availability of data and materials

It has been reported and cited in the methodology part of the manuscript.

### Ethics approval and consent to participate

Not applicable in this section



**Consent for publication**

Not applicable in this section

**Competing interests**

Not applicable in this section

**Author details**

<sup>1</sup>Chemistry Department, Ahmadu Bello University, Zaria, Kaduna State 810107, Nigeria. <sup>2</sup>Chemistry Department, Baze University, Abuja, Nigeria. <sup>3</sup>Science Education Department, Ajasin University, Akungba Akoko, Ondo State, Nigeria.

Received: 12 June 2020 Accepted: 20 July 2020

Published online: 08 August 2020

**References**

- Adeniji SE, Arthur DE, Abdullahi M, Haruna A (2020b) Quantitative structure–activity relationship model, molecular docking simulation and computational design of some novel compounds against DNA gyrase receptor. *Chem Africa*. <https://doi.org/10.1007/s42250-020-00132-9>
- Adeniji SE, Shallangwa GA, EArthur D, Abdullahi M, Mahmoud AY, Haruna A (2020c) Quantum modelling and molecular docking evaluation of some selected quinoline derivatives as anti-tubercular agents. *Heliyon* 6:e03639
- Adeniji SE, Uba S, Uzairu A (2018) Theoretical modeling and molecular docking simulation for investigating and evaluating some active compounds as potent anti-tubercular agents against MTB CYP121 receptor. *Future J Pharm Sci* 4:284–295
- S.E. Adeniji, S. Uba, A. Uzairu, A derived QSAR model for predicting some compounds as potent antagonist against mycobacterium tuberculosis: a theoretical approach, *Hindawi Advances in Preventive Medicine* (2019), Article ID 5173786.
- Adeniji SE, Uba S, Uzairu A (2020a) Multi-linear regression model, molecular binding interactions and ligand-based design of some compounds against Mycobacterium tuberculosis. *Network Mod Anal Health Inform Bioinform* 9:1–18
- Adeniji SE, Uba S, Uzairu A (2020d) Theoretical modeling for predicting the activities of some active compounds as potent inhibitors against Mycobacterium tuberculosis using GFA-MLR approach. *J King Saud Univ Sci* 32:575–586
- Guan LP, Jin QH, Tian GR, Chai KY, Quan ZS (2007) Synthesis of some quinoline-2 (1H)-one and 1, 2, 4-triazolo[4, 3 -a] quinoline derivatives as potent anticonvulsants. *J Pharm Sci* 10:254–262
- Gujjar R, Marwaha A, White J, White L, Creason S, Shackelford DM, Baldwin J, Charman WN (2009) Identification of a metabolically stable triazolopyrimidine-based dihydroorotate dehydrogenase inhibitor with activity in mice. *J Med Chem* 52:1864–1872
- Hafez HN, Abbas HA, El-Gazzar AR (2008) Synthesis and evaluation of analgesic, anti-inflammatory and ulcerogenic activities of some triazolo- and 2-pyrazolylpyrido[2,3-d]- pyrimidines. *Acta Pharma* 58:359–378
- Holla BS, Mahalinga M, Karthikeyan MS, Poojary B, Akberali PM, Kumari NS (2005) Synthesis, characterization and anti-microbial activity of some substituted 1, 2, 3-triazoles. *Eur J Med Chem* 40:1173–1178
- Huang YY, Deng JY, Gu J, Zhang ZP, Maxwell A, Bi LJ, Chen YY, Zhou YF, Yu ZN, Zhang XE (2006) The key DNA-binding residues in the Cterminal domain of Mycobacterium tuberculosis DNA gyrase A subunit (GyrA). *Nucleic Acids Res* 34:5650–5659
- Ibrahim MT, Uzairu A, Shallangwa GA, Uba S (2020) In-silico activity prediction and docking studies of some 2, 9-disubstituted 8-phenylthio/ phenylsulfanyl-9 h-purine derivatives as anti-proliferative agents. *Heliyon* 6:e03158
- James CW (2009) DNA entanglement and the action of the DNA topoisomerases. Cold Spring Harbor Laboratory Press, Cold Spring Harbor, p 245
- Patel NB, Khan IH, Rajani SD (2010) Pharmacological evaluation and characterizations of newly synthesized 1,2,4-triazoles. *Eur J Med Chem* 45
- Piton J, Petrella S, Delarue M, André-Leroux G, Jarlier V, Aubry A, Mayer C (2010) Structural insights into the quinolone resistance mechanism of Mycobacterium tuberculosis DNA gyrase. *PLoS ONE* 5:e12245. <https://doi.org/10.1371/journal.pone.0012245>
- J. Piton, S. Petrella, M. Delarue, G. André-Leroux, V. Jarlier, A. Aubry, C. Mayer, Structural insights into the quinolone resistance mechanism of Mycobacterium tuberculosis DNA gyrase, <https://www.rcsb.org/structure/3IFZ>.

- Roy K, Chakraborty P, Mitra I, Ojha PK, Kar S, Das RN (2011) Some case studies on application of “rm2” metrics for judging quality of quantitative structure–activity relationship predictions: emphasis on scaling of response data. *J. Comput. Chem.* 34 (2013) 1071–1082. QSAR models-strategies and importance. *Int J Drug Des Discov* 3:511–519
- Tropsha A, Gramatica P, Gombar VK (2003) The importance of being earnest: validation is the absolute essential for successful application and interpretation of QSPR models. *Mol Inform* 22:69–77
- W.H.O (2018) <http://www.who.int/news-room/fact-sheets/detail/tuberculosis>
- Zhang Y, Post-Martens K, Denkin S (2006) New drug candidates and therapeutic targets for tuberculosis therapy. *Drug Discov Today* 11:21–27

**Publisher’s Note**

Springer Nature remains neutral with regard to jurisdictional claims in published maps and institutional affiliations.

**Submit your manuscript to a SpringerOpen® journal and benefit from:**

- Convenient online submission
- Rigorous peer review
- Open access: articles freely available online
- High visibility within the field
- Retaining the copyright to your article

Submit your next manuscript at ► [springeropen.com](https://www.springeropen.com)